Laser and Particle Beams (2002), *20*, 177–184. Printed in the USA.

DOI: 10.1017/S0263034602202049

Electron–ion collision-induced harmonics generation in a plasma with an isotropic bi-Maxwellian distribution

G. FERRANTE,[1] S.A. URYUPIN,[2] AND M. ZARCONE[1]

[1]Istituto Nazionale per la Fisica della Materia and Dipartimento di Fisica e Tecnologie Relative, Viale delle Scienze, 90128 Palermo, Italy
[2]P.N. Lebedev Physical Institute, Leninsky pr. 53, 117924, Moscow, Russia

(RECEIVED 16 November 2001; ACCEPTED 16 December 2001)

Abstract

A treatment is given of harmonics generation resulting from nonlinear inverse bremsstrahlung in a plasma with an anisotropic bi-Maxwellian electron velocity distribution function. A complete characterization of the process is reported. In particular, analytically and numerically we established how the efficiency of the odd harmonics generation and their polarization depend on such process parameters as: (1) the degree of effective temperature anisotropy, (2) the frequency and the intensity of the fundamental wave, and (3) the angle between the fundamental wave field direction and the symmetry axis of the electron distribution function.

Keywords: Bremsstrahlung; Electron-ion collisions; Harmonics; Laser Field

1. INTRODUCTION

Collisions of electrons with ions in the presence of a strong electromagnetic field are one of the basic mechanisms for harmonics generation in fully ionized plasmas (Silin, 1965, 1999*a*). The harmonics generation characteristics typical of this mechanism depend both on the properties of the pump field (Silin, 1998; Ferrante *et al*., 2000), and on the shape of the electron distribution function (EDF) of the plasma (Silin, 1999*b*; Ferrante *et al*., 2001*a*). In particular, in investigating the influence of the EDF shape on the process of harmonics generation, one can consider the case when the pump field itself forms the nonequilibrium EDF either as result of atom ionization (Silin, 1999*b*, 1999*c*), or as a result of electron anisotropic heating due to inverse bremsstrahlung (Ferrante *et al*., 1997, 2001*b*). In such a case, the orientation of the anisotropic EDF axes depends obviously in a definite way on the external radiation field parameters. In the present article, we consider a different case, in which there is no link between the initial shape of the EDF and the acting radiation parameters. In other words, we assume that an anisotropic bi-Maxwellian EDF is preliminarily created by a strong ultrashort laser pulse, either through atom tunnel ionization (Delone & Krainov, 1991), or due to electron heating during inverse bremsstrahlung absorption of the pulse (Chichkov *et al*., 1992). After the laser pulse–plasma interaction, the newly formed anisotropic bi-Maxwellian EDF lasts for a time interval of the order of the inverse of the effective electron collision frequency.

Below we investigate the basic properties of harmonics generation due to nonlinear inverse bremsstrahlung in such a prepared anisotropic plasma, when the latter interacts with a linearly polarized pump laser field. In the following section, we give the derivation of the general expression for the harmonics generation efficiency during electron–ion collisions in the presence of a linearly polarized high-frequency radiation field, interacting with a plasma exhibiting an anisotropic bi-Maxwellian EDF. The distribution is taken such that $T_z > T_\perp$, where T_z and $T_\perp$ are, respectively, the electron effective temperatures along and perpendicular to the EDF symmetry axis. We give also the general expression for the deviation angle of the harmonic field with respect to the pump field direction. The reason for the deviation of the harmonic field is traced back to the plasma conductivity anisotropy at different harmonic frequencies. The general expression for the harmonic generation efficiency is analyzed in Section 3. Taking as an instance the harmonic 3ω, we obtain simple asymptotic expressions of its generation efficiency and perform the corresponding numerical calculations. For odd harmonics of higher orders, we report numerical calculations of generation efficiency versus (1) the

Address correspondence and reprint requests to: Michelangelo Zarcone, Istituto Nazionale per la Fisica della Materia and Dipartimento di Fisica e Tecnologie Relative, Viale delle Scienze, 90128 Palermo, Italy. E-mail: zarcone@unipa.it

electron temperature degree of anisotropy, (2) the frequency and the intensity of the pump field, and (3) the angle between the pump field and the EDF symmetry axis. For a highly anisotropic plasma, when $T_z \gg T_\perp$, we evidence a strong anisotropy in the harmonic generation efficiency, which manifests itself in both relatively weak and strong pump fields. In Section 4 we investigate the possible dependences of the deviation angle of the harmonic field with respect to the pump field direction. For the deviation angle of the third harmonic, we derive clear asymptotic expressions, taking particularly simple forms when the temperature anisotropy is not large. For the case when $T_z \gg T_\perp$, we show that the 3ω harmonic field exhibits a large deviation angle. For the third, as well as for higher order odd harmonics, numerical calculations are carried out to illustrate how the deviation angle depends on the angle between the pump field and the symmetry axis of the initial EDF. Calculations are carried out for different values of the ratio $T_z/T_\perp$ and of the pump field parameters.

2. BASIC EQUATIONS

As it is now established (see, e.g., Delone & Krainov, 1991), in atom tunnel ionization by a linearly polarized radiation, a velocity photoelectron distribution is formed which is close to an anisotropic bi-Maxwellian EDF with the effective electron temperature along the field T_z larger than the temperature perpendicular to it $T_\perp$. That is, the velocity photoelectron distribution to a good approximation is given by

$$F(\vec{v}) = \frac{Nm}{2\pi T_\perp}\sqrt{\frac{m}{2\pi T_z}}\exp\left[-\frac{mv_\perp^2}{2T_\perp} - \frac{mv_z^2}{2T_z}\right], \tag{1}$$

where m is the electron mass, N is the electron density, and $T_\perp$ and T_z are the effective temperatures in energy units. A distribution close to the anisotropic bi-Maxwellian EDF is also formed in the case of anisotropic electron heating as a result of inverse bremsstrahlung absorption of intense electromagnetic radiation when the amplitude of the electron quiver velocity v_E exceeds the initial thermal velocity v_T, but is smaller than Zv_T, where Z is the multiplicity of ionization of plasma ions (for details, see Chichkov *et al.*, 1992; Ferrante *et al.*, 2001*b*). Let us assume that a plasma with an anisotropic bi-Maxwellian EDF is preliminarily formed as a result of one of the two processes quoted above. Below, we investigate how such a prepared plasma will interact with a high frequency electromagnetic wave, created by some other source of coherent electromagnetic radiation. Let us take the wave field in the form

$$\vec{E}\cos(\omega t - \vec{k}\vec{r}), \tag{2}$$

where the frequency and the wave vector are linked by the dispersion relation

$$\omega^2 = \omega_L^2 + k^2c^2, \tag{3}$$

where c is the speed of light, $\omega_L^2 = 4\pi e^2 N/m$ is the square of the electron plasma frequency, and e is the electron charge. Without loss of generality, we assume that the electric field vector has only two components, along and perpendicular to the EDF symmetry axis $\vec{E} = (E_x, 0, E_z)$.

As result of electron scattering by ions, the field (2) generates in the plasma harmonics of the current at the odd frequencies $(2n+1)\omega$, where $n = 0, 1, 2, \ldots$. Assuming, as usual in the theory of inverse bremsstrahlung (Silin, 1965, 1998, 1999*a*, 1999*b*, 1999*c*; Ferrante *et al.*, 1997, 2000, 2001*a*) that the influence of the relatively rare collisions on the electron motion in the high-frequency field (2) may be treated as perturbation, for the time derivative of the current density proportional to the collision frequency, from the kinetic equation we find

$$\frac{\partial}{\partial t}\delta\vec{j} = -\frac{1}{\pi^2}eNv_E^3\nu(v_E)\int d\vec{q}\,\frac{\vec{q}}{q^2}\sum_{n=0}^{\infty}J_{2n+1}(\vec{q}\vec{v}_E) \times \exp\left[-q_z^2\frac{T_z}{2m} - q_\perp^2\frac{T_\perp}{2m}\right]\sin[(2n+1)(\omega t - \vec{k}\vec{r})], \tag{4}$$

where J_{2n+1} is the Bessel function of order $2n+1$, $v_E = |\vec{v}_E|$, $\vec{v}_E = e\vec{E}/m\omega$ is the amplitude of electron quiver velocity, and $\nu(v_E)$ is the effective electron–ion collision frequency,

$$\nu(v_E) = \frac{4\pi Ze^4N}{m^2v_E^3}\Lambda, \tag{5}$$

and Λ is the field-dependent Coulomb logarithm (see Silin & Uryupin, 1981, for more details). In accordance with (4), the current density $\delta\vec{j}$ has the form

$$\delta\vec{j} = \sum_{n=0}^{\infty}\delta\vec{j}_n(\vec{r}, t). \tag{6}$$

The harmonics of the current density $\delta\vec{j}_n(\vec{r}, t)$ with $n \neq 0$ yield the generation of the corresponding harmonics of the field at the frequencies $(2n+1)\omega$. To determine the electric fields of the harmonics $\vec{E}_n(\vec{r}, t)$ with $n \neq 0$, we use the Maxwell equations, where the current $\delta\vec{j}_n(\vec{r}, t)$ is the source of the harmonics. Taking into account the condition

$$\nabla\cdot\vec{E}_n(\vec{r}, t) = 0, \tag{7}$$

from the Maxwell equations we have

$$c^2\Delta\vec{E}_n(\vec{r}, t) - \frac{\partial^2\vec{E}_n(\vec{r}, t)}{\partial t^2} - \omega_L^2\vec{E}_n(\vec{r}, t) = 4\pi\frac{\partial}{\partial t}\delta\vec{j}_n(\vec{r}, t). \tag{8}$$

We look for a solution of the linear equation (8) in the form

$$\vec{E}_n(\vec{r}, t) = -\vec{E}_n\sin[(2n+1)(\omega t - \vec{k}\vec{r})]. \tag{9}$$

Then, taking into account the expressions (4) and (6) and the dispersion relation (3), from (8) we obtain the electric field of the nth harmonics resulting from nonlinear inverse bremsstrahlung

$$\vec{E}_n = \frac{1}{\pi n(n+1)} \frac{eN}{\omega_L^2} v_E^3 \nu(v_E) \int d\vec{q}\, \frac{\vec{q}}{q^2} J_{2n+1}(\vec{q}\vec{v}_E) \times \exp\left[-q_z^2 \frac{T_z}{2m} - q_\perp^2 \frac{T_\perp}{2m}\right], \quad (10)$$

where $n \neq 0$. According to (10), the field of the harmonic $\vec{E}_n$, similar to that of the fundamental field $\vec{E}$, has only two components E_{nx} and E_{nz}. The efficiency of generation of the $(2n+1)\omega$ harmonic is characterized by the ratio

$$\eta_n = \left|\frac{E_n}{E}\right|^2. \quad (11)$$

Using (10), the generation efficiency is written as

$$\eta_n = \left[\frac{\nu(v_T)}{\omega}\right]^2 a^2(n,\gamma,\delta,\alpha). \quad (12)$$

In (12) the following notations are used:

$$v_T = \sqrt{T/m}, \qquad T = (T_z + 2T_\perp)/3, \qquad \delta = \Delta/T,$$
$$\Delta = T_z - T_\perp > 0, \qquad \gamma = m v_E^2/4T; \quad (13)$$

further α is the angle between the field $\vec{E}$ and the oZ axis, while the function $a(n) = a(n,\gamma,\delta,\alpha)$ is given by the relations

$$a^2(n) = a_x^2 + a_z^2, \quad (14)$$

$$\begin{Bmatrix} a_x(n) \\ a_z(n) \end{Bmatrix} = \frac{1}{2\pi\sqrt{2\pi}\, n(n+1)} \int_0^1 \frac{dy}{\sqrt{1-y^2}} \times \int_{-1}^{1} dx \begin{Bmatrix} y\sqrt{1-x^2} \\ x \end{Bmatrix} \times \frac{(x\cos\alpha + y\sqrt{1-x^2}\sin\alpha)}{\left[1+\delta\left(x^2 - \frac{1}{3}\right)\right]^{3/2}} \times \exp[-W]\{I_n[W] - I_{n+1}[W]\} \quad (15)$$

$$W = \frac{\gamma}{1+\delta\left(x^2-\frac{1}{3}\right)}[x\cos\alpha + y\sqrt{1-x^2}\sin\alpha]^2, \quad (16)$$

where I_n is the modified Bessel function of n-order. As the harmonics generation efficiency depends on the angle between the fundamental field $\vec{E}$ and the EDF symmetry axis, the direction of the harmonics polarization, in general, will not coincide with the direction of the fundamental field polarization. To determine the angle $\Psi(n) = \Psi(n,\gamma,\delta,\alpha)$ of the vector $\vec{E}_n$ with respect to the vector $\vec{E}$, it is natural to exploit the relation

$$\Psi(n,\gamma,\delta,\alpha) = \arccos\left(\frac{\vec{E}\vec{E}_n}{|\vec{E}||\vec{E}_n|}\right) \equiv \arccos[G(n,\gamma,\delta,\alpha)], \quad (17)$$

where the function $G(n,\gamma,\delta,\alpha)$ has the form

$$G(n,\gamma,\delta,\alpha) = \frac{1}{2\pi\sqrt{2\pi}\, a n(n+1)} \int_0^1 \frac{dy}{\sqrt{1-y^2}} \times \int_{-1}^{1} dx \frac{(x\cos\alpha + y\sqrt{1-x^2}\sin\alpha)^2}{\left[1+\delta\left(x^2-\frac{1}{3}\right)\right]^{3/2}} \times \exp[-W]\{I_n[W] - I_{n+1}[W]\}. \quad (18)$$

The functions $a^2(n,\gamma,\delta,\alpha)$ and $\Psi(n,\gamma,\delta,\alpha)$ define both the efficiency and the polarization direction of higher harmonics versus (1) γ, characterizing the intensity of the fundamental wave; (2) δ, defining the degree of anisotropy of the initial EDF; and (3) the angle α, defining the direction of the polarization vector of the fundamental field with respect to the initial anisotropic bi-Maxwellian EDF symmetry axis. All these dependencies will analyzed below in the next two sections.

3. HARMONICS GENERATION EFFICIENCY

In this section, we consider the harmonics generation efficiency in a plasma with the anisotropic bi-Maxwellian EDF (1). In particular, as an instance, we consider the third harmonic ($n = 1$ and frequency 3ω), for which we derive asymptotic expressions. The basic features of generation of higher order harmonics and of the 3ω harmonic as well are reported below in graphical form. Let us start with the case when the pump field is weak enough that

$$T_z > T_\perp \gg m v_E^2. \quad (19)$$

Then, keeping in (15) only the terms linear in γ (or in W), from (14) approximately we have

$$a^2(1) = \frac{2}{\pi}\left(\frac{m v_E^2}{16 T_\perp}\right)^2 \left(\frac{T_z + 2T_\perp}{12 T_z}\right)^3 \times \left\{\left[\frac{T_z}{2T_\perp}\sin^2\alpha + (1-3g)\left(\cos^2\alpha - \frac{1}{4}\sin^2\alpha\right)\right]^2 \times \sin^2\alpha + [2g\cos^2\alpha + (1-3g)\sin^2\alpha]^2\cos^2\alpha\right\}, \quad (20)$$

https://doi.org/10.1017/S0263034602202049 Published online by Cambridge University Press

where

$$g = \frac{T_z T_\perp}{(T_z - T_\perp)^2}\left(\frac{\sqrt{T_z}}{2\sqrt{T_z - T_\perp}}\ln\frac{\sqrt{T_z} + \sqrt{T_z - T_\perp}}{\sqrt{T_z} - \sqrt{T_z - T_\perp}} - \frac{4T_z - T_\perp}{3T_z}\right). \tag{21}$$

Expression (20) takes a very simple form in a plasma with isotropic EDF, that is, when $T_z = T_\perp = T$. In fact, from (20) we have

$$a^2(1) = \frac{1}{2\pi}\left(\frac{mv_E^2}{160T}\right)^2, \tag{22}$$

which does not depend on the angle α. If instead $T_z > T_\perp$, then the efficiency of the third harmonic generation depends on α. The generation efficiency is largest at $\alpha = \pi/2$, when the pump field lies in the plane of the smaller temperate $T_\perp$. In fact, it is just in this plane that the electron–ion collision frequency has its largest value, and, accordingly, the harmonics generation as well is in this plane the most effective, thanks to the nonlinear inverse bremsstrahlung. On the contrary, at $\alpha = 0$ (or $\alpha = \pi$) the function $a^2(1)$ has a minimum, physically arising from the small values of the collision frequency characteristic of electrons with temperature T_z. The larger the ratio $T_z/T_\perp$, the stronger the anisotropy in harmonics generation. Let us consider now the 3ω harmonic generation in a strong field, when

$$mv_E^2 \gg T_z > T_\perp. \tag{23}$$

When these inequalities are obeyed, one can neglect the corrections due to the electron thermal motion along the pump field direction. Exploiting this circumstance from (12)–(16) approximately we find

$$\begin{aligned}\eta_1 = {} & \left(\frac{3}{4\pi}\right)^2\left[\frac{\nu(v_E)}{\omega}\right]^2 \\ & \times\left\{\left(\ln\left[\frac{mv_E^2}{(\sqrt{T_\perp} + \sqrt{T_z\sin^2\alpha + T_\perp\cos^2\alpha})^2}\right] - C_3\right)^2\right. \\ & + \frac{4\sin^2\alpha\cos^2\alpha}{T_z\sin^2\alpha + T_\perp\cos^2\alpha} \\ & \left.\times\frac{(T_z - T_\perp)^2}{(\sqrt{T_\perp} + \sqrt{T_z\sin^2\alpha + T_\perp\cos^2\alpha})^2}\right\},\end{aligned} \tag{24}$$

where C_3 is a constant of unity order

$$\begin{aligned}C_3 = {} & \frac{\sqrt{2\pi}}{3}\int_0^\infty dy\sqrt{y}e^{-y} \\ & \times\ln y\{y[I_o(y) - I_3(y)] + 3(1-y)[I_1(y) - I_2(y)]\} \\ \simeq {} & 0.62.\end{aligned} \tag{25}$$

We note that expressions (24) and (25) have been obtained in the approximation when $\ln\xi - C_3 > 0$, where ξ indicate the argument of the logarithm entering in (24). From (24) it follows, that for α values near $\pi/2$, the function η_1 has a local minimum. This behavior is specific to the strong field limit. In a weak field, as can be seen from (20), at $\alpha = \pi/2$, the 3ω harmonic generation efficiency has its maximum value. For values of α approaching zero (or π) the behavior of the function η_1 depends on the relation between the quantities $T_z/T_\perp - 1 > 0$ and $\ln(mv_E^2/4T_\perp) - C_3 > 0$. When the degree of the temperature anisotropy is relatively not large, such that

$$\frac{T_z}{T_\perp} - 1 < \ln\left(\frac{mv_E^2}{4T_\perp}\right) - C_3, \tag{26}$$

the function η_1 has a local maximum. On the contrary, when the degree of anisotropy is so large that the inequality reverse to (26) takes place, η_1 has another local minimum. In such conditions, the third harmonic generation is the most effective, if the pump field is directed at an angle $\alpha_m \neq \pi/2$ with respect to the EDF symmetry axis. In particular, for $T_z \gg T_\perp$, the maximum of the function η_1 is reached at $\alpha_m \sim \sqrt{T_\perp/T_z} \ll 1$ (or at $\pi - \alpha_m$). For a strongly anisotropoic plasma, another interesting limiting case may be envisaged when

$$T_z \gg mv_E^2 \gg T_\perp. \tag{27}$$

Together with the r.h.s inequality (27), we assume that the following stronger inequality too is fulfilled:

$$mv_E^2\sin^2\alpha \gg T_\perp. \tag{28}$$

For small α (or close to π), inequality (28) does not hold, and for the third harmonic generation, we may use expression (20), adequate for weak fields. For conditions corresponding to inequalities (27) and (28), from (12)–(16) we have

$$\eta_1 = \left[\frac{\nu(v_E)}{\omega}\right]^2\left[\frac{mv_E^2}{8\pi T_z}\right]\frac{1}{\sin^2\alpha}. \tag{29}$$

Expression (29) has a minimum at $\alpha = \pi/2$. As α departs from $\pi/2$, the 3ω harmonic generation efficiency grows up to its maximum at $\alpha_m \sim \sqrt{T_\perp/mv_E^2} \ll 1$ (or for $\pi - \alpha_m$). The further departure of α from $\pi/2$ gives a decreasing of generation efficiency according to (20), which corresponds to the weak field limit.

In Figure 1, the function $a^2(1)$ (12) is plotted. The function $a^2(1)$ describes the efficiency of the third harmonic generation in a plasma with $T_z = 10T_\perp$ (or $\delta = 9/4$) versus α, the angle between the field of the pump wave and the oZ-axis. Different curves correspond to different values of the parameter γ (13): 0.1, 0.4, 1, 3, 10. The curve with $\gamma = 0.1$ corresponds to the weak field limit, and like expression (20),

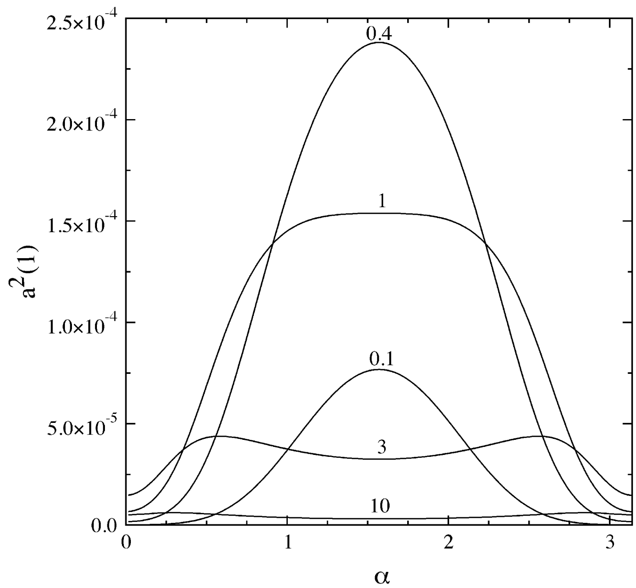

Fig. 1. The 3ω harmonic generation efficiency $a^2(1)$ versus α, the angle between the field of the pump wave and the oZ-axis. The five curves correspond to $\delta = 9/4$ ($T_z = 10T_\perp$) and five values of the parameter γ: 0.1, 0.4, 1, 3, 10.

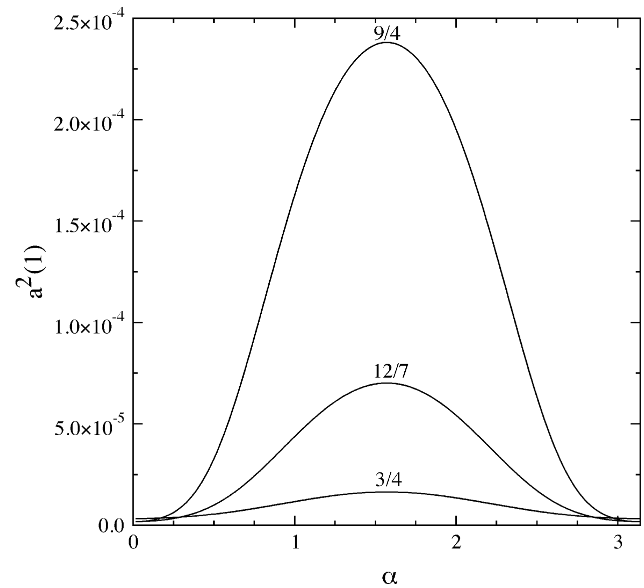

Fig. 2. The same function as in Figure 1, but for $\gamma = 0.4$ and three values of the parameter δ: $\delta = 9/4$ ($T_z = 10T_\perp$), $\delta = 12/7$ ($T_z = 5T_\perp$), $\delta = 3/4$ ($T_z = 2T_\perp$).

shows a strong anisotropy of the function $a^2(1)$ with a large maximum for $\alpha = \pi/2$. For $\gamma = 0.4$, the efficiency of the third harmonic generation at $\alpha = \pi/2$ reaches its maximum. The generation efficiency at $\alpha = \pi/2$ decreases with a further increasing of γ. This is shown by the curves with $\gamma = 1, 3, 10$. The maximum of generation efficiency shifts in the region of angles close to $\alpha = 0$ and $\alpha = \pi$. The last property is illustrated clearly by the curve with $\gamma = 3$. A similar behavior takes place also at $\gamma = 10$, but for values of α very close to zero or to π. The curve for $\gamma = 10$ as well as the asymptotic formula (24) show a weak dependence of $a^2(1)$ versus α in the strong field limit.

In Figure 2, the function $a^2(1)$ versus the angle α is plotted for $\gamma = 0.4$ and for three different values of the parameter δ (13): 9/4 ($T_z = 10T_\perp$), 12/7 ($T_z = 5T_\perp$,), 3/4 ($T_z = 2T_\perp$). According to Figure 2, the higher the temperature ratio $T_z/T_\perp$, the larger the anisotropy of the third harmonic generation efficiency. For instance, at $\delta = 9/4$ ($T_z = 10T_\perp$), the degree of anisotropy is characterized by a factor of 25.

Similar dependences take place for higher harmonics also. In Figure 3, the generation efficiency of the fifth 5ω ($n = 2$), the seventh 7ω ($n = 3$) and the ninth 9ω ($n = 4$) harmonics are plotted for $\delta = 9/4$ ($T_z = 10T_\perp$) and for two values of the parameter γ: 3 and 10. From Figure 1 and Figure 3, one sees a qualitative similarity of the functions $a^2(n)$, but an essential difference too is noted. Namely, the degree of anisotropy of the functions $a^2(n)$ is increasing with the harmonic order. This effect is more pronounced for relatively weak fields. In particular, according to the dashed curves in Figure 3, for $\gamma = 3$ the values of the functions $a^2(3)$ and $a^2(4)$ vary by two and three orders, respectively. The degree of anisotropy of the functions $a^2(n)$ decreases with the increasing of γ. This property is clearly seen from the comparison of the continuous ($\gamma = 10$) and dashed ($\gamma = 3$) curves in Figure 3. For a strong field, the anisotropy becomes logarithmically weak. For higher harmonic order, the transition to the strong limit takes place at larger field values.

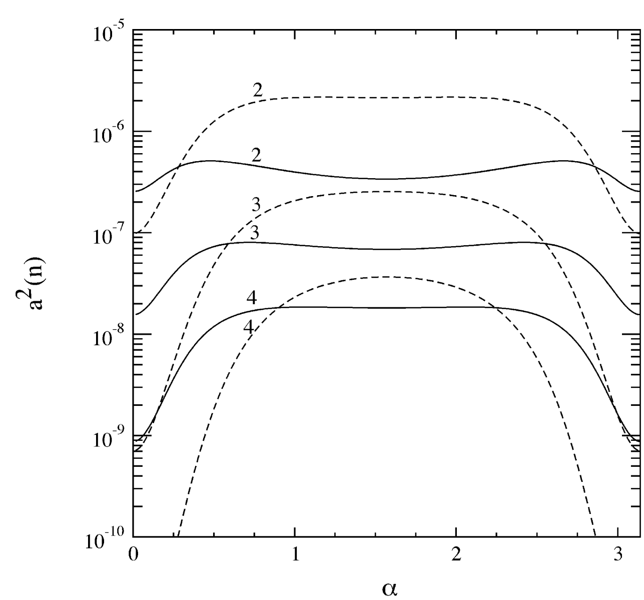

Fig. 3. Efficiency of harmonics generation $a^2(n)$ versus α, the angle between the field of the pump wave and the oZ-axis, in a plasma with $\delta = 9/4$ ($T_z = 10T_\perp$). Different curves correspond to harmonics 5ω ($n = 2$), 7ω ($n = 3$), 9ω ($n = 4$). Dashed curves correspond to $\gamma = 3$ and continuous lines to $\gamma = 10$.

https://doi.org/10.1017/S0263034602202049 Published online by Cambridge University Press

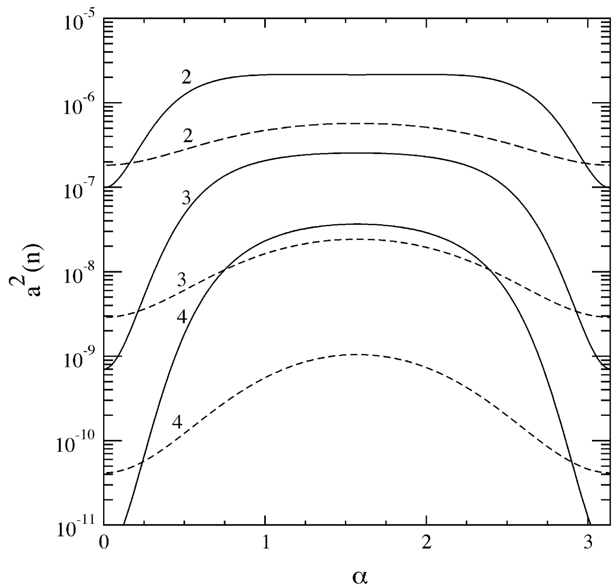

Fig. 4. The same function as in Figure 3, but for $\gamma = 3$ and two values of the parameter δ: $\delta = 9/4$ ($T_z = 10T_\perp$)—continuous curves; $\delta = 3/4$ ($T_z = 2T_\perp$)—dashed curves.

Figure 4, where the dependencies of the functions $a^2(n)$ on the angle α for $\gamma = 3$ and for $\delta = 9/4$ ($T_z = 10T_\perp$) and $\delta = 3/4$ ($T_z = 2T_\perp$) are plotted, shows that the harmonics generation anisotropy increases with increasing of the ratio between the longitudinal and the transverse electron temperatures. Besides, Figure 4 shows a large increasing of the anisotropy of the function $a^2(n)$ when the ratio $T_z/T_\perp$ increases by a factor of 5. The effect of the anisotropy amplification is more pronounced for high harmonic orders.

4. HARMONICS POLARIZATION

Due to the anisotropy of plasma conductivity at the harmonics frequencies, deviation of the harmonics field with respect to the pump field direction takes place. According to the treatment given in Section 2, the value of the deviation angle Ψ depends on the harmonic order, the degree of temperature anisotropy, the intensity of the pump wave, and is also a function of the angle formed by the pump field direction and the EDF symmetry axis. Below, we report some simple asymptotic expressions of the function $\Psi(1) = \Psi(1,\gamma,\delta,\alpha)$, defining the deviation angle of the third harmonic field. In the case of weak fields, when inequality (19) holds, from (18) we find

$$\Psi(1) = \arctan(F), \tag{30}$$

$$F = \frac{1 - 5g + \left[\dfrac{T_z}{2T_\perp} - \dfrac{5}{4}(1-3g)\right]\tan^2\alpha}{2g + (1-3g)\tan^2\alpha + \tan^2\alpha\left[(1-3g)\left(1 - \dfrac{1}{4}\tan^2\alpha\right) + \dfrac{T_z}{2T_\perp}\tan^2\alpha\right]}\tan\alpha, \tag{31}$$

where the function g is given by (21). If the temperature anisotropy is not large,

$$1 - \frac{T_\perp}{T_z} \ll 1, \tag{32}$$

expression (31) significantly simplifies, and (30) takes the form

$$\Psi(1) = \frac{5}{7}\left(1 - \frac{T_\perp}{T_z}\right)\sin\alpha\cos\alpha. \tag{33}$$

According to (30), (31), and (33) there is no deviation of the polarization vector of the third harmonic at $\alpha = \pi/2$ and $\alpha = 0$ (or $\alpha = \pi$). From (33), it follows that in the case of weak anisotropy, the largest deviation of the polarization vector takes place at $\alpha = \pi/4$. Instead, if $T_z \gg T_\perp$, in accordance with (30) and (31), for the deviation angle, we have approximately $\Psi(1) = \pi/2 - \alpha$.

In the case of a strong pump field, when inequalities (23) take place, from (18), we have an expression like (30), but with the function F weakly depending (through a logarithm) on the pump field intensity

$$F = \frac{2\sin\alpha\cos\alpha}{\sqrt{T_\perp} + \sqrt{T_z\sin^2\alpha + T_\perp\cos^2\alpha}}\,\frac{T_z - T_\perp}{\sqrt{T_z\sin^2\alpha + T_\perp\cos^2\alpha}} \times\left\{\ln\left[\frac{mv_E^2}{(\sqrt{T_\perp} + \sqrt{T_z\sin^2\alpha + T_\perp\cos^2\alpha})^2}\right] - C_3\right\}^{-1}, \tag{34}$$

Eq. (34) has been obtained in the approximation, when the logarithm in the denominator is much larger than $C_3 \simeq 0.62$. If the temperature anisotropy is small (see inequality (32)), then from (30) and (34), we have approximately

$$\Psi(1) = \left(1 - \frac{T_\perp}{T_z}\right)\frac{\sin\alpha\cos\alpha}{\left[\ln\left(\dfrac{mv_E^2}{4T_z}\right) - C_3\right]}. \tag{35}$$

In (35) the dependence of $\Psi(1)$ on α is similar to that found for the weak field case (33). For large values of the temperature anisotropy, $T_z \gg T_\perp$, and for not particularly small angles, $\alpha \gg \sqrt{T_\perp/T_z}$, from (34) follows

$$F \simeq \frac{2\sin\alpha\cos\alpha}{\ln\left(\dfrac{mv_E^2}{T_z\sin^2\alpha}\right) - C_3}. \tag{36}$$

https://doi.org/10.1017/S0263034602202049 Published online by Cambridge University Press

Expressions (30) and (36) give a dependence on α similar to that of (35), but the numerical values of the angle Ψ may result significantly larger.

Finally, we consider another limiting case of strong anisotropy. When inequalities (27) and (28) hold, from (18) we have approximately

$$\Psi(1) \simeq \frac{\pi}{2} - \alpha. \tag{37}$$

This last result is similar to that obtained in the limit of weak field for a plasma with $T_z \gg T_\perp$.

In addition to the relatively simple formulas (30)–(37) for the deviation angle $\Psi(n)$, we report numerical results as well. In Figure 5, the dependences of the deviation angle are plotted for the third harmonic $\Psi(1)$ in a plasma with $\delta = 9/4$ ($T_z = 10T_\perp$) and for few values of the parameter γ: 0.4, 1, 3, 10. For the selected values of γ and δ, according to Figure 5, the deviation angle of the 3ω harmonics reaches its maximum value at $\alpha \sim \pi/6$ (or $\sim 5\pi/6$). For $\gamma = 0.4$ the maximum value of $\Psi(1)$ is $\sim\pi/4$. With γ increasing, the maximum value of $\Psi(1)$ is decreasing up to $\Psi(1) \sim \pi/6$ for $\gamma = 10$. Similar dependencies of the function $\Psi(1)$ versus the angle α are plotted in Figure 6, for $\gamma = 0.4$ and for three values of anisotropy parameter δ: 9/4 ($T_z = 10T_\perp$), 12/7 ($T_z = 5T_\perp$), 3/4 ($T_z = 2T_\perp$). From Figure 6, one can see how the value of the angle $\Psi(1)$ decreases with the temperature anisotropy decreasing. At the same time, the maximum value of the function $\Psi(1)$ shifts to the region of angles close to $\pi/4$, which is realized in a plasma with weak anisotropy. We note that, already for the value $\delta = 3/4$ ($T_z = 2T_\perp$), the function $\Psi(1)$ in Figure 6 is approximated by the asymptotic formula (33) rather well. Similar polarization properties for higher harmonics are illustrated in Figure 7 and Figure 8. The deviation angles of the fifth ($n = 2$), seventh ($n = 3$), and ninth ($n = 4$) harmonics for a plasma with $\delta = 9/4$ ($T_z = 10T_\perp$) are plotted in Figure 7. Dashed curves correspond to pump wave with $\gamma = 3$, while continuous curve corresponds to $\gamma = 10$. As well as for the 3ω harmonic (see Fig. 5), small values of the deviation angle

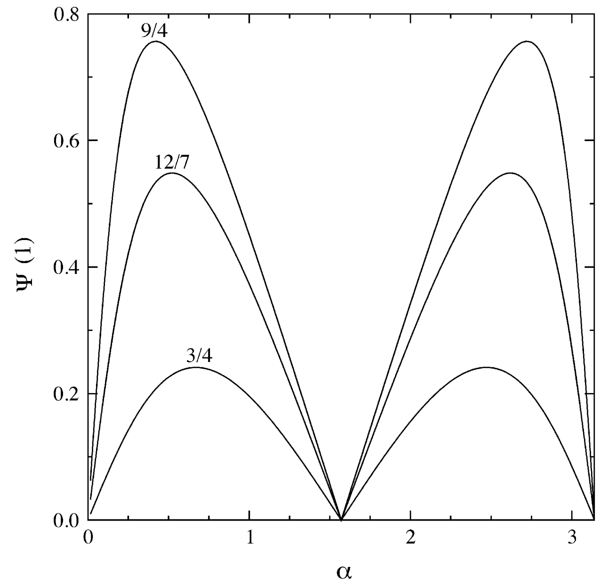

Fig. 6. The same function as in Figure 5, but for $\gamma = 0.4$ and three values of the parameter δ: $\delta = 9/4$ ($T_z = 10T_\perp$), $\delta = 12/7$ ($T_z = 5T_\perp$), $\delta = 3/4$ ($T_z = 2T_\perp$).

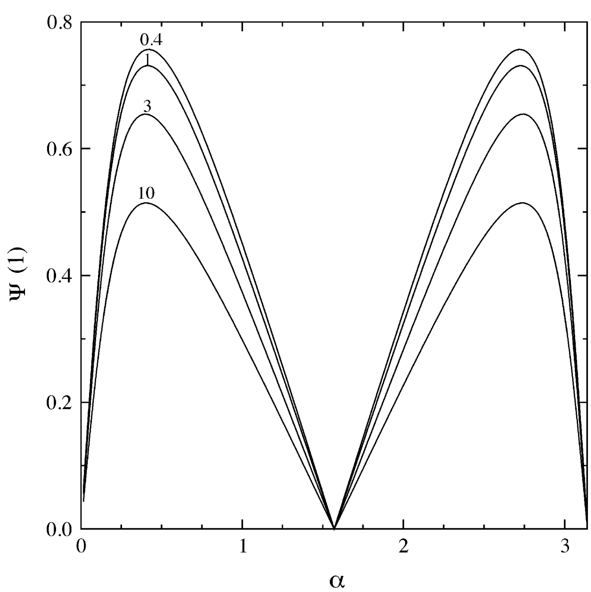

Fig. 5. Deviation angle of the 3ω harmonic field versus α, the angle between the field of the pump wave and the EDF symmetry axis, in a plasma with $\delta = 9/4$ ($T_z = 10T_\perp$). The curves correspond to four values of the parameter γ: 0.4, 1, 3, 10.

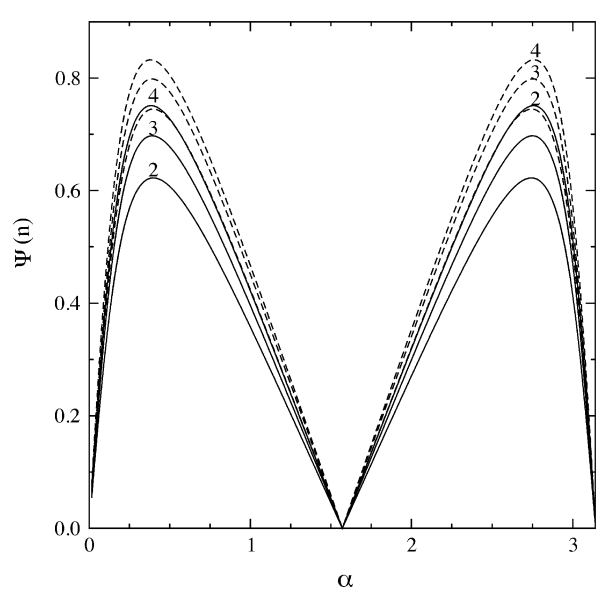

Fig. 7. Deviation angle of the fifth ($n = 2$), seventh ($n = 3$) and ninth ($n = 9$) harmonics $\Psi(n)$ versus α in a plasma with $\delta = 9/4$ ($T_z = 10T_\perp$). Dashed curves correspond to $\gamma = 3$ and continuous lines to $\gamma = 10$.

https://doi.org/10.1017/S0263034602202049 Published online by Cambridge University Press

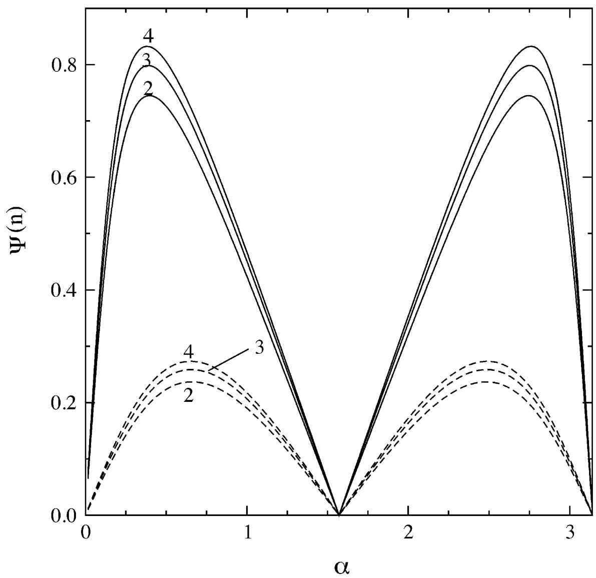

Fig. 8. The same functions as in Figure 7, but for $\gamma = 3$ and two values of the parameter δ. Dashed curves correspond to $\delta = 3/4$ ($T_z = 2T_\perp$) and continuous lines to $\delta = 9/4$ ($T_z = 10T_\perp$).

correspond to large values of the parameter γ. Further, the decrease of the electron temperature anisotropy is found to lead to the decrease of the function $\Psi(n)$. This statement is illustrated in Figure 8, where for $\gamma = 3$, the functions $\Psi(n)$, with $n = 2, 3, 4$ are plotted for a plasma with $\delta = 9/4$ ($T_z = 10T_\perp$) and $\delta = 3/4$ ($T_z = 2T_\perp$). As well as for the third harmonic 3ω (see Fig. 6), one can see a sizable decreasing of the functions $\Psi(n)$, with $n = 2, 3, 4$, which is connected with the decreasing of the temperature anisotropy. The shift of the deviation angle in the region of α close to $\pi/4$ also takes place.

5. CONCLUSIONS

We have presented a treatment of the harmonics generation taking place during nonlinear inverse bremsstrahlung in a plasma exhibiting an anisotropic bi-Maxwellian electron distribution function. It has allowed us to establish, analytically and numerically, a number of basic properties of this highly nonlinear process of laser–plasma interaction. In particular, our main concern has been to elucidate how the harmonics generation efficiency and the harmonics polarization depend on the plasma and pump field parameters. The reported results are expected to prove useful for optimization of the conditions able to yield generation of high order harmonics and for diagnosing the anisotropy of the EDF itself. Though the results have been obtained for a plasma exhibiting a bi-Maxwellian EDF, they are of general character and open the avenue of the treatment of anisotropy effects in plasmas with more complicated initial EDF, which may result from different physical processes, such as, for instance, atoms ionization or plasma interaction with quasi-stationary strong fields.

ACKNOWLEDGMENTS

This work was supported by the International Science and Technical Center (project N.1253), the Russian Fund for Basic Research (project N99-02-18075) and the Russian-Italian Agreement for Scientific Collaboration. The authors wish to acknowledge also the support by the Italian Ministry for University and Technology (MURST, ex-40%), and by the Palermo University through the International Relations Fund.

REFERENCES

Chichkov, B.N., Shumsky, S.A. & Uryupin, S.A. (1992). Nonstationary electron distribution functions in a laser field. *Phys. Rev. A* **45**(10), 7475–7479.

Delone, N.B. & Krainov, V.P. (1991). Energy and angular electron spectra for the tunnel ionization of atoms by strong low-frequency radiation. *J. Opt. Soc. Am. B* **8**(6), 1207–1211.

Ferrante, G., Zarcone, M. & Uryupin, S.A. (2000). Harmonic generation and wave mixing in a plasma enacted by two linearly polarized laser fields. *J. Opt. Soc. Am. B* **17**(8), 1383–1389.

Ferrante, G., Zarcone, M. & Uryupin, S.A. (2001*a*). Electron heating anisotropy and harmonics generation in a plasma. *Proc. Int. Conf. Laser 2000*, pp. 215–220. McLean, VA: STS Press.

Ferrante, G., Zarcone, M. & Uryupin, S.A. (2001*b*). Electron distribution functions in laser fields. *Plasma Sources Sci. Technol.* **10**, 318–328.

Ferrante, G., Zarcone, M., Uryupin, S.A. & Porshnev, P.I. (1997). Harmonic generation in a plasma with laser-heated electron velocity distributions. *J. Opt. Soc. Am. B* **14**(7), 1716–1722.

Silin, V.P. (1965). Nonlinear high-frequency plasma conductivity. *Sov. Phys. JETP* **20**(6), 1510–1516.

Silin, V.P. (1998). On coherent harmonics bremsstrahlung in laser plasma. *JETP* **87**(3), 468–477.

Silin, V.P. (1999*a*). On the coherent bremsstrahlung generation of harmonics in a laser-produced plasma. *Quantum Electron.* **26**(1), 11–18.

Silin, V.P. (1999*b*). On the generation of harmonics in a tunnel-photoionized plasma. *Quantum Electron.* **27**(3), 253–256.

Silin, V.P. (1999*c*). Generation of high-order harmonics in the photoionization of gas. *Quantum Electron.* **29**(10), 49–55.

Silin, V.P. & Uryupin, S.A. (1981). Absorption of intense electromagnetic radiation in collisions of charged particles. *JETP* **54**(9), 485–492.